Eur. Phys. J. AP 1, 87–91 (1998)

THE EUROPEAN PHYSICAL JOURNAL
APPLIED PHYSICS

Estimating a conductivity distribution *via* a FEM-based nonlinear Bayesian method*

T. Martin[a] and J. Idier

Laboratoire des Signaux et Systèmes[b], Plateau de Moulon, 91192 Gif-sur-Yvette Cedex, France

Received: 20 March 1997 / Revised: 4 September 1997 / Accepted: 2 October 1997

Abstract. *Electrical Impedance Tomography* (EIT) of closed conductive media is an ill-posed inverse problem. In order to solve the corresponding direct problem, the *Finite Elements Method* (FEM) provides good accuracy and preserves the non linear dependence of the observation set upon the conductivity distribution. In this paper, we show that the Bayesian approach presented in [1] for linear inverse imaging problems is also valid for a non linear problem such as EIT. Our contribution is based on an edge-preserving Markov model as prior for conductivity distribution. *Maximum a posteriori* reconstruction results from 40 dB noisy measurements (simulated with a finer mesh) yield significant resolution improvement compared to classical methods.

PACS. 02.60.Lj Ordinary and partial differential equations; boundary value problems – 02.60.Pn Numerical optimization – 02.70.Dh Finite-element and Galberkin methods

1 Introduction

Electrical Impedance Tomography (EIT) of closed conductive media with steady currents is a non-invasive imaging technique that aims at estimating the impedance distribution within a conductive body from electrical measurements on the surface. Applications can be found in medical imaging and non-destructive testing. Usually, thanks to surface electrodes, the experiment consists in injecting currents in the body and measuring the surface voltage distributions. Here, we deal with 2D reconstructions.

In EIT, the first difficulty consists in finding an accurate direct model. Indeed, the image-data relation derived from Maxwell formulas, is ruled by a second order partial derivative equation which yields no analytical solution for arbitrary domain shape or arbitrary conductivity distribution. Therefore, one has to approximate the direct problem. The desired accuracy of the direct solver has to be checked through three kind of errors [2]:

- *mathematical modeling error:* this error occurs from the difference between the actual physical behavior and the mathematical model. Here, according to the well-known Maxwell equation accuracy, this error reduces to uncertainties resulting from 2D and steady current hypotheses (since low-frequency currents are used in most EIT experiments);
- *discretization error:* theoretical distance between the exact solution of the mathematical model and the approximation;
- *round-off errors:* loss of accuracy due to the limitations of computing machines.

Analytic approximations [3,4] reveal too simplified domain-shapes to provide satisfactory accuracy for arbitrary domain. Thus, many authors [5,6] preferred linear approximations. However, if the sought distribution is highly contrasted (which is often the case in EIT applications), linearized models are no longer valid. Following [7–9], we opted for a *Finite Element Method* (FEM) direct model (Sect. 2). Indeed, it provides a natural capability to match the shape of the domain as well as good convergence properties towards the true solution. Thus, not only discretization and round-off errors are low but also the non linear dependence of the observations upon the conductivity distribution is preserved. If finer modelisation is sought, FEM may also easily incorporate some specific electrode models. Besides, this technique is frequently used for many problems involving Partial Differential Equations (PDE), in such fields as electrostatics, solid or fluid mechanics... It also reveals as suited to a Bayesian approach of the inversion.

The second (and major) difficulty of EIT is its intrinsic ill-posed character [10]. Actually, some internal conductivity change have nearly no consequence on the output voltage distribution. This ill-posedness was ignored by the first reconstruction methods [5] based on simple backprojection techniques. As well as other methods developed so far, they provide estimators that are very sensitive to noise

* This paper was presented at NUMELEC'97.

[a] e-mail: martin@lss.supelec.fr

[b] CNRS-SUPÉLEC-UPS

(even with a SNR above 70 dB), for lack of regularization analysis.

In this paper, we adopted the Bayesian regularizing approach of [1] and we introduce prior knowledge (mainly smoothing properties) on the sought conductivity distribution *via* a probability distribution. In order to reconstruct an image of *log-conductivity* elements within the 2D domain (where each element is a triangle from the FEM mesh system), we consider a neighborhood system compatible with the mesh system. This allows the introduction of a *Markov Random Field* (MRF) as a prior model for log-conductivity. In our simulations, we use a non convex original domain with an intermediary contrasted conductivity distribution and a 40 dB signal-to-noise ratio (which is severe in EIT). The *Maximum A Posteriori* (MAP) reconstruction results, obtained through the optimization of the posterior likelihood criterion, yield significant resolution improvement compared to classical methods. Moreover, to get more realistic observation sets, we use 2 different FEM direct models: the first, with a finer domain discretization, is used to generate the observed voltage outputs while the second, with a coarser resolution, is dedicated to the MAP estimation method.

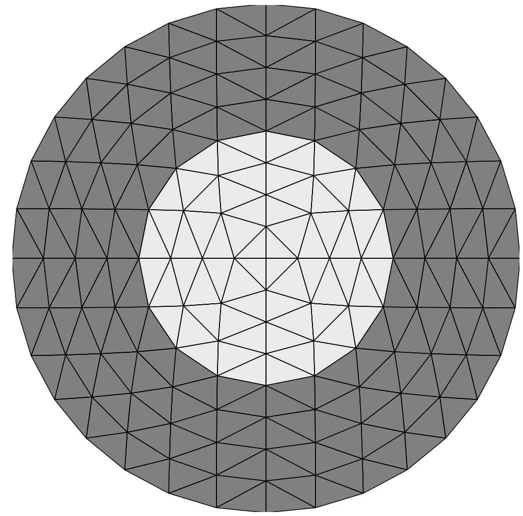

Fig. 1. Conductivity distribution.

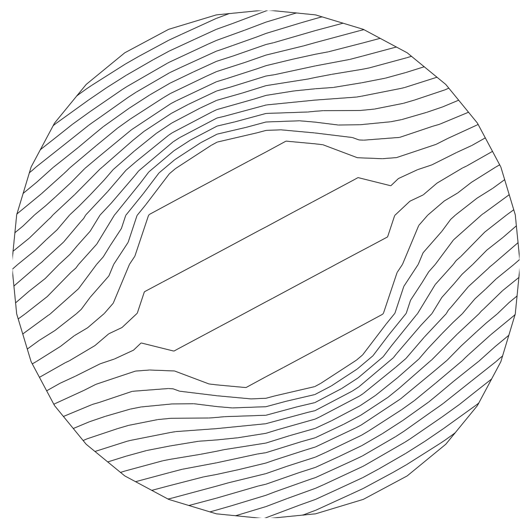

Fig. 2. Equipotential lines. On a circular domain with a centered circular discontinuity, the existent analytic solution allows to check the accuracy of the FEM direct solver. The example above contains an intermediary number of elements (256) and the input current distribution is a 1-period sine function. The equipotential lines are numerically found straight within the discontinuity area, as stated by the analytic results.

2 FEM for the resolution of the direct problem

Let us call Ω the 2D domain and $\bar{\Omega}$ its border. We respectively note I (A), V (V) the current stream and voltage distributions on Ω and $\bar{I}$, $\bar{V}$ the same distributions restricted on $\bar{\Omega}$. These scalar distributions are defined, up to a constant, by $\mathbf{E} = -\mathbf{grad}\ V$ where $\mathbf{E}$ is the electric field and by $\mathbf{j} = (\mathbf{grad}\ I)^{\perp}$ (true in 2D only) where $\mathbf{j}$ is the current field and $(x, y)^{\perp} = (-y, x)$. Lastly, we call σ the conductivity distribution. On one hand, the direct problem consists in finding $\bar{V}$ from $\bar{I}$ and σ, while the inverse problem requires the determination of σ from $\bar{I}$ and $\bar{V}$.

The observation model is described by the PDE $\mathrm{div}(\sigma \mathbf{grad}\ V) = 0$, along with adequate additive current boundary conditions. In the general case, there exists no analytical solution for this PDE. When linear approximations are too rough, the equivalent following variational formulation of the problem (Ref. [11])

$$\frac{1}{2}\iint_{\Omega}[\sigma|\mathbf{grad}\ V|^2 + \sigma^{-1}|\mathbf{grad}\ I|^2]\mathrm{d}x\mathrm{d}y + \int_{\bar{\Omega}} V\frac{\partial \bar{I}}{\partial \mathbf{t}}\mathrm{d}s = 0$$

can be discretized with the Finite Element Method [7–9] (more precisely with the Raleigh-Ritz method [11]). The discretization of the problem amounts to divide the domain into, say P elements defining N nodes on Ω, among which $\bar{N}$ are on the border $\bar{\Omega}$. Thereafter, the discretized observation model reads:

$$\bar{\boldsymbol{v}} = \boldsymbol{P}\boldsymbol{A}_{\boldsymbol{\sigma}}^{-1}\boldsymbol{P}^{\top}\boldsymbol{D}\bar{\boldsymbol{\imath}}, \tag{1}$$

where $\bar{\boldsymbol{v}}$ and $\bar{\boldsymbol{\imath}}$ (of size $\bar{N}$, *i.e.* the number of border nodes) are discretized counterparts of $\bar{V}$ and $\bar{I}$. The vector $\boldsymbol{\sigma}$ contains the P elements of conductivity. $\boldsymbol{A}_{\boldsymbol{\sigma}}$ is the $(N-1)\times(N-1)$ "stiffness" matrix of the problem defined by:

$$a_{ij} = \sum_{n\in e(i)\cap e(j)} \sigma_n\ \theta(i, j, n), \tag{2}$$

where $e(i)$ is the set of neighboring elements of node i and $\theta(i, j, p)$ depends on the geometric features of the mesh on Ω (details can be found in [11] or some other general reference book about FEM). $\boldsymbol{A}_{\boldsymbol{\sigma}}$ is positive-definite and very sparse: in practice, more than 98% of its entries are null. $\boldsymbol{P}$ is merely a $\bar{N}\times(N-1)$ border projection operator and $\boldsymbol{D}$ is a difference operator defined by:

$$(\boldsymbol{D}\bar{\boldsymbol{\imath}})_n = \bar{\boldsymbol{\imath}}_{n+1} - \bar{\boldsymbol{\imath}}_{n-1} \bmod \bar{N}, \tag{3}$$

i.e., the current stream difference measured between the two neighbors of the n-th border node.

The matrix $\boldsymbol{A}_{\boldsymbol{\sigma}}$ linearly depends on $\boldsymbol{\sigma}$, so the FEM image-data relation (Eq. (1)) is a *non linear* function of the conductivity distribution. Actually, in our FEM discretization, current streams and voltages are approximated by piecewise linear functions on each element, whose nodal values are respectively the components of $\bar{\boldsymbol{\imath}}$ and $\bar{\boldsymbol{v}}$ while conductivity is approximated through piecewise constant functions whose element values belong to $\boldsymbol{\sigma}$.

This method is known to have a $\mathrm{O}(r^2)$ convergence rate towards the true solution, where r is the largest element diameter [11]. However, prior accuracy estimates are difficult to obtain. Computed simulations, in cases where analytic solutions are available [3] (*cf.* Figs. 1 and 2) show that the magnitude of the *solution error* (sum of discretization error and round-off error) is lower than 40 dB. Thus, the FEM direct model need not be refined nor regularized. An increase of the polynomial order of the FEM approximations of I, V and σ, which would be computationally more expensive than a mesh refinement, is neither desirable.

3 A Bayesian MAP estimation method

The knowledge of $\bar{\boldsymbol{\imath}}$ $(\bar{N} \times 1)$ and $\boldsymbol{\sigma}$ $(P \times 1)$ allows to compute $\bar{\boldsymbol{v}}$ $(\bar{N} \times 1)$. Somehow, there exists no straight inverse way to get $\boldsymbol{\sigma}$ from the observation. First of all, since we have $\bar{N} < N < P$, the number of data $\bar{N}$ is lower than the number of unknowns P. In practice, K independent observation sets are gathered, with $K > P/\bar{N}$, so that classical backprojection techniques are implementable [5,8]. Such methods aim at minimizing the quadratic distance between the observations and the FEM direct simulation. Yet, these methods provide no acceptable results. This is not surprising since, we guess, a small change on inner conductivity has very few influence on the observation on the border. On the other hand, given the ill-posed character of the inverse problem, the backprojected image may rather depict amplified noise rather than true conductivity values.

In 1991, Hua *et al.* [9] proposed to add a quadratic penalty term to the usual criterion. Its stabilizing effect is well-known and provides robust conductivity maps, but at the expense of poor resolution. Here we propose to introduce another kind of penalty term, corresponding to a non-Gaussian Markov prior probability from the Bayesian point of view. Following Barber and Brown [4], the use of the log-conductivity $\gamma = \log(\sigma)$ is preferred. Unlike σ, it need not be constrained positive. Besides, the mapping $\bar{\boldsymbol{v}}(\boldsymbol{\gamma})$ looks closer to linearity than $\bar{\boldsymbol{v}}(\boldsymbol{\sigma})$. Both features make the penalized criterion easier to optimize with respect to γ.

If we consider a centered white Gaussian noise $\bar{\boldsymbol{n}}^k$ of variance λ^2, for the K direct observation models $k = 1, \ldots, K$:

$$\bar{\boldsymbol{v}}^k = \boldsymbol{P}\boldsymbol{A}_{\boldsymbol{\sigma}}^{-1}\boldsymbol{P}^\top \boldsymbol{D}\bar{\boldsymbol{\imath}}^k + \bar{\boldsymbol{n}}^k, \tag{4}$$

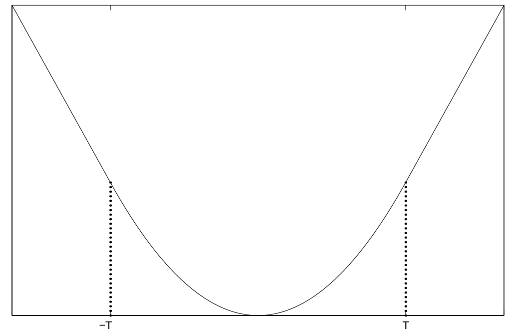

Fig. 3. The Huber function $h_{\mathrm{T}}(t)$.

we get the likelihood:

$$p(\bar{\boldsymbol{v}}^k|\boldsymbol{\gamma};\bar{\boldsymbol{\imath}}^k) \propto \exp\left[-\frac{1}{2\lambda^2}\sum_{k=1}^{K}|\bar{\boldsymbol{v}}^k - \boldsymbol{P}\boldsymbol{A}_{\exp\boldsymbol{\gamma}}^{-1}\boldsymbol{P}^\top \boldsymbol{D}\bar{\boldsymbol{\imath}}^k|^2\right]. \tag{5}$$

In EIT applications, especially in medical imaging, conductivity distributions are often homogeneous areas, separated by discontinuities. Therefore, we suggest to use the 2D mesh structure itself to introduce a MRF as prior. Let $v(p)$ be the set of spatial neighbors of the p-th element ($v(p)$ contains three elements at most), and let us introduce the $\mathcal{C}^1$ convex Huber penalty function defined by:

$$h_{\mathrm{T}}(t) := \begin{cases} t^2 & \text{if } |t| < T, \\ 2T|t| - T^2 & \text{otherwise} \end{cases}$$

and the prior probability $p(\boldsymbol{\gamma}) = \exp(-\varPhi_{\mathrm{T}}(\boldsymbol{\gamma}))$, with

$$\varPhi_{\mathrm{T}}(\boldsymbol{\gamma}) = \frac{1}{2}\sum_{p=1}^{P}\sum_{q\in v(p)} h_{\mathrm{T}}(\gamma_p - \gamma_q). \tag{6}$$

$h_{\mathrm{T}}(\gamma_p - \gamma_q)$ favours local smoothness thanks to its parabolic zone, but it also allows discontinuities detection between pixels thanks to its linear parts [12] (*cf.* Fig. 3).

From the Bayes rule, the posterior probability density is given by:

$$p(\boldsymbol{\gamma}|\bar{\boldsymbol{v}}^k;\bar{\boldsymbol{\imath}}^k) \propto p(\bar{\boldsymbol{v}}^k|\boldsymbol{\gamma};\bar{\boldsymbol{\imath}}^k)p(\boldsymbol{\gamma}). \tag{7}$$

As a result, computing the MAP estimate amounts to minimizing the following criterion:

$$J(\boldsymbol{\gamma}) = \sum_{k=1}^{K}\|\bar{\boldsymbol{v}}^k - \boldsymbol{P}\boldsymbol{A}_{\exp\boldsymbol{\gamma}}^{-1}\boldsymbol{P}^\top \boldsymbol{D}\bar{\boldsymbol{\imath}}^k\|^2 + 2\lambda^2\varPhi_{\mathrm{T}}(\boldsymbol{\gamma}). \tag{8}$$

This criterion is the sum of a non convex likelihood term and a prior convex term. The latter reduces the global non convexity of $J(\boldsymbol{\gamma})$, so it favours its minimization, even toward a local minimum. Hua *et al.*, who introduced a white Gaussian regularization term with respect to $\boldsymbol{\sigma}$, used a Newton-Raphson method to minimize their criterion. This second order algorithm is computationaly heavy because it requires Hessian approximation, and looks inadequate because the criterion has not a parabolic shape. We preferred a first order descent method: the conjugate gradient algorithm, which proves simpler and faster.

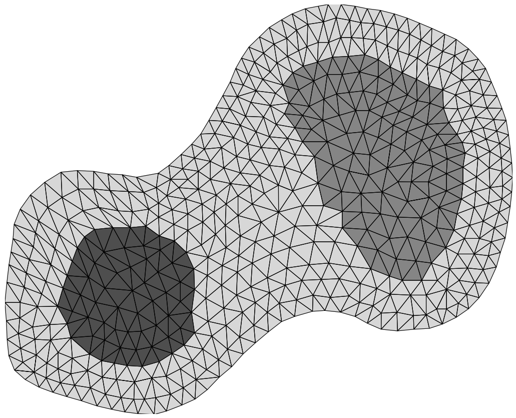

Fig. 4. Original conductivity distribution.

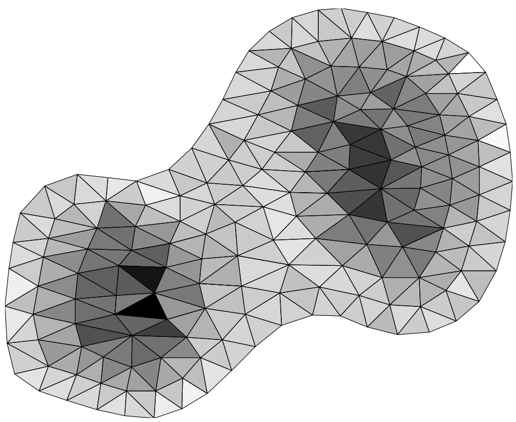

Fig. 5. Reconstruction with no regularization.

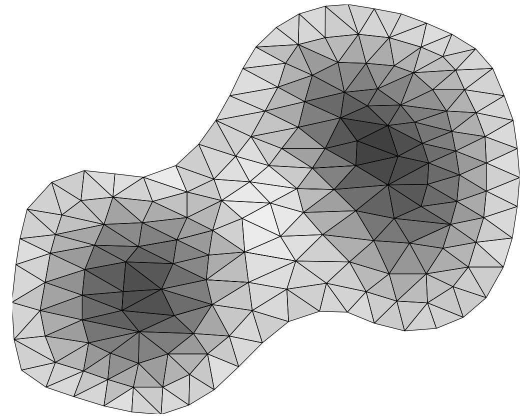

Fig. 6. Gauss-Markov prior reconstruction.

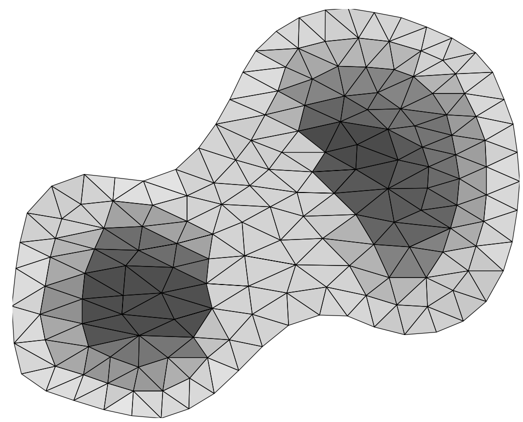

Fig. 7. Huber-Markov prior reconstruction.

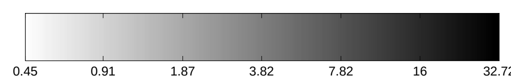

Fig. 8. Scale used for the conductivity distribution.

4 Simulated estimation results

Here, we present the simulated reconstruction results obtained on a "peanut shape" domain. For the construction of the original conductivity and the data outputs, the domain was discretized into $N = 552$ nodes, $\bar{N} = 100$ border nodes and $P = 1002$ elements. Its conductivity consists of a homogeneous background of 1 $\mathrm{S\,m^{-1}}$, with two discontinuous areas of 6 $\mathrm{S\,m^{-1}}$ and 20 $\mathrm{S\,m^{-1}}$ (*cf.* Fig. 1). For the reconstruction, we took $N = 174$, $P = 296$ and the $\bar{N} = 50$ border points which are chosen as every second point of the finely discretized border. The $K = 7 > P/\bar{N}$ different current and voltage distributions are sampled from the original border distribution in the same way. The current stream inputs are chosen as successive rotations of the same 3-level piecewise constant distribution. As mentioned above, the voltage observation sets have a 40 dB SNR.

Like many authors, we choose, as the starting point of our minimization algorithm, the measurable uniform background conductivity of the original distribution [9]. We present here the results obtained with three different reconstruction methods: the first is obtained without regularization, the second with a quadratic (Markov-Gauss) regularization and the third is the proposed method. Hyperparameters λ for the quadratic term and $(\lambda,\ T)$ for the Huber function were chosen empirically to get the best qualitative reconstruction results but the reconstruction quality is not very sensitive to their variations (order of magnitude variations are necessary to detect significant influence on the reconstruction result).

Table 1. Comparisons between execution times and discrepancy measures $\delta_1(\gamma,\ \hat{\gamma})$ (where γ is the original distribution and $\hat{\gamma}$ is the estimated distribution), for the 3 different estimation methods.

Method	λ	T	$\delta_1(\gamma,\hat{\gamma})$	Exec. Time
No regul.	0	∞	0.70	248 s
Gaussian	0.012	∞	0.64	244 s
Huber	1.5	10^{-5}	0.53	1415 s

In order to compare the quality of the reconstructions $\hat{\boldsymbol{\gamma}}$, we measure the $\mathcal{L}^1$ distance of the estimated distribution to the original. Indeed, the $\mathcal{L}^1$ norm is known to be in good agreement with visual appreciation. More precisely, we use the following discrepancy measure: $\delta_1(\gamma,\hat{\gamma}) = ||\gamma-\hat{\gamma}||_1/||\gamma||_1$, where $\gamma,\hat{\gamma}$: $\Omega \longrightarrow \mathbb{R}$ are respectively the distributions associated with the vectors $\gamma, \hat{\gamma}$.

The Table 1 and the reconstructions (*cf.* Figs. 5, 6 and 7) show that regularization is not only useful but necessary, and that the convex Huber function is relevant for the reconstruction of discontinuities.

References

1. G. Demoment, IEEE ASSP **37**, 2024 (1989).
2. H. Kardestuncer, D.H. Norrie, F. Brezzi, *Finite Element Handbook* (McGraw-Hill Book Company, New York, 1987).
3. David Isaacson, IEEE Trans. Medical Imaging **5**, 91 (1986).
4. D. Barber, B. Brown, *Recent developments in applied potential tomography*, APT Information Processing in Medical Imaging pp. 106–121 (1986).
5. M. Tasto, H. Schomberg, *Object reconstruction from projections and some non-linear extensions*, Pattern Recognition and Signal Processing, edited by C.H. Chen, pp. 485–503 (1978).
6. C. Cohen-Bacrie, *Régularisation du problème inverse de tomographie d'impédance électrique*, Master's thesis, École polytechnique de Montréal, 1994.
7. J.G. Webster, *Electrical Impedance Tomography* (Adam Hilger, IOP Publishing Ltd, 1990).
8. R.V. Kohn, A. McKenney, *Numerical implementation of a variational method for electrical impedance tomography*, Inverse Problems, pp. 389–414 (1990).
9. P. Hua, E.J. Woo, J.G. Webster, W.J. Tompkins, IEEE Trans. Med. Imag., 621 (1991).
10. G. Alessandrini, Applicable Analysis **27**, 153 (1988).
11. A.J. Davies, *The Finite Element Method: A First Approach* (Oxford Applied Mathematics and Computing Science Series, 1980).
12. P. Huber, *Robust Statistics* (John Wiley & Sons, New York, 1981).